Dynamically Feasible Trajectory and Open-Loop Control Design for Unmanned Airships

Filoktimon Repoulias and Evangelos Papadopoulos, *Senior Member, IEEE*

National Technical University of Athens, Department of Mechanical Engineering, 15780 Athens, Greece

{firepoul, egpapado}@central.ntua.gr

Abstract—**This paper describes a method for planning six DOF trajectories for an underactuated unmanned airship and for computing the open-loop controls. Beginning with a smooth inertial 3D trajectory to be tracked by the center of mass of the vehicle, the proposed algorithm, based on the dynamics of the system, provides the 3D corresponding body-fixed linear and angular velocities and the vehicle orientation, yielding a feasible 6 DOF trajectory. The derived trajectory is further used to compute the three available open-loop controls. Since the variables of the trajectory are consistent with the vehicle's dynamics, a closed-loop tracking controller can significantly improve its performance incorporating these variables. Furthermore, examining the resulting open-loop controls, the designer can judge about the capability of the actuators to meet the requirements of tracking the specific trajectory.**

I. INTRODUCTION

Unmanned, robotic (autonomous) airships, see Fig. 1, belong to the category of Unmanned Air Vehicles (UAVs) that play an increasingly significant role in surveillance, monitoring, and transportation [1]. They are employed in various missions such as observation of urban areas or the battlefields, fire detection, rescue, science, even in planetary exploration [2]. They also present a useful experimental platform for testing inertial navigation, positioning, and visual sensors, actuators and complex control algorithms since almost always such vehicles are underactuated, i.e., they have more degrees of freedom than control inputs. Although robotic airships have some advantages against the rest of the UAVs at low speeds and low altitude applications [3], they too present a challenging control problem: underactuation imposes non-integrable acceleration constraints. Furthermore, their kinematic and dynamic models are highly nonlinear and coupled, making control design a hard task. Underactuation rules out the use of customary control schemes e.g. full state-feedback linearization, and the complex (aero)dynamics excludes designs based solely on kinematic models.

Trajectory tracking is a frequently assigned task to a robotic airship which requires the design of control laws that guide the vehicle to track an inertial trajectory, i.e., a 3D path on which a time law is specified. The performance of trajectory tracking controllers is greatly improved when trajectory planning has been designed previously.

The goal of trajectory planning is to generate the
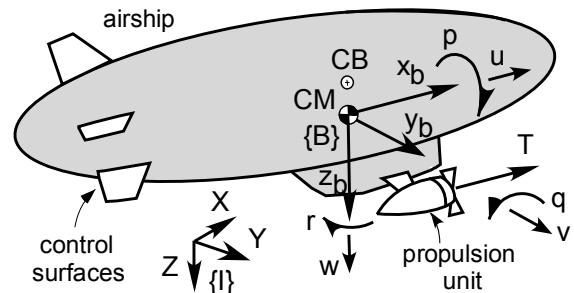
Figure 1. The robotic airship with the controls and motion variables.

reference inputs to the motion control system which ensures that the vehicle executes the planned trajectory. While several researchers have addressed the hovering, visual, and trajectory tracking control problem for UAVs and robotic airships, see for example [4], [5], [6], to the best of the authors' knowledge, there is no known work that studied the trajectory planning for underactuated UAVs in 3D motion. A first result on the subject of trajectory planning was presented in our previous works, [7] and [8], where we studied the problem of trajectory planning for an Autonomous Underwater Vehicle.

In this paper, we describe a method for planning six DOF trajectories for an underactuated unmanned airship and for computing the open-loop controls. Beginning with a smooth inertial 3D trajectory to be tracked by the center of mass (CM) of the vehicle, the proposed algorithm, based on the dynamics of the system, provides the 3D corresponding body-fixed linear and angular velocities and the vehicle orientation, yielding a feasible 6 DOF trajectory. The derived trajectory is further used to compute the three available open-loop controls required to follow the trajectory. Finally, simulation results are presented to demonstrate the effectiveness of the algorithm.

II. AIRSHIP DYNAMICS AND KINEMATICS

In this section, the kinematic and dynamic equations of motion for a robotic airship moving in 3D space are presented.

To describe the kinematics, two reference frames are employed, the inertial reference frame $\{I\}$ and a body-fixed frame $\{B\}$, see Fig. 1. As shown in this figure, the origin of $\{B\}$ frame coincides with the airship center of mass (CM) while the center of buoyancy (CB) is on the

negative z_b body axis for static stability. Using the standard notation of aeronautical engineering, the general motion of the airship in 6 DOF can be described by the following vectors:

$$\mathbf{\eta}=[\mathbf{\eta}_1^T,\mathbf{\eta}_2^T]^T;\quad \mathbf{\eta}_1=[x,y,z]^T;\quad \mathbf{\eta}_2=[\phi,\theta,\psi]^T;$$
$$\mathbf{v}=[\mathbf{v}_1^T,\mathbf{v}_2^T]^T;\quad \mathbf{v}_1=[u,\upsilon,w]^T;\quad \mathbf{v}_2=[p,q,r]^T; \quad (1)$$

In (1), $\mathbf{\eta}_1$ denotes the inertial position of the CM and $\mathbf{\eta}_2$ the orientation of $\{B\}$ – in terms of Euler angles – with respect to the $\{I\}$ frame. Vector $\mathbf{v}_1$ denotes the linear velocity of the CM and $\mathbf{v}_2$ the angular velocity of $\{B\}$ with respect to $\{I\}$ frame, both expressed in the body-fixed $\{B\}$ frame. In guidance and control applications, for the representation of rotations, it is customary to use the $x-y-z$ (roll-pitch-yaw) convention defined in terms of Euler angles adopted in the present work or quaternions. Hence, the velocity transformation between $\{B\}$ and $\{I\}$ frames is expressed as

$$\dot{\mathbf{\eta}}_1=\mathbf{J}_1(\mathbf{\eta}_2)\mathbf{v}_1 \quad (2)$$

where

$$\mathbf{J}_1(\mathbf{\eta}_2)=\begin{bmatrix} c\psi c\theta & -s\psi c\phi+c\psi s\theta s\phi & s\psi s\phi+c\psi c\phi s\theta \\ s\psi c\theta & c\psi c\phi+s\phi s\theta s\psi & -c\psi s\phi+s\theta s\psi c\phi \\ -s\theta & c\theta s\phi & c\theta c\phi \end{bmatrix} \quad (3)$$

The body-fixed angular velocities and the time rate of the Euler angles are related through

$$\dot{\mathbf{\eta}}_2=\mathbf{J}_2(\mathbf{\eta}_2)\mathbf{v}_2 \quad (4)$$

where

$$\mathbf{J}_2(\mathbf{\eta}_2)=\begin{bmatrix} 1 & s\phi t\theta & c\phi t\theta \\ 0 & c\phi & -s\phi \\ 0 & s\phi/c\theta & c\phi/c\theta \end{bmatrix} \quad (5)$$

where $s\cdot=\sin(\cdot)$, $c\cdot=\cos(\cdot)$, $t\cdot=\tan(\cdot)$.

The dynamic model of the airship used for the illustration of the method is taken from the study of [3] and [4]. It is a simplified model developed for control design tasks, which captures the main dynamical characteristics of an unmanned airship moving in 3D space, see Fig. 1. Modeling inaccuracies can be treated as small and bounded disturbances that along with external disturbances, such as air gusts, can be compensated for by a robust closed-loop tracking controller. The vehicle is underactuated, i.e., it has less control inputs than the number of DOF. Regarding the means of propulsion and actuation the following features are used:

Aerodynamic control surfaces like rudders and elevators to control yaw and pitch motions respectively, Fig. 1.

Vectored thrust, meaning the rotation of the propulsion units about an axis parallel to the body– y_b axis so as to provide thrust in the direction required. In this way, pitch torque control is achieved, see Fig. 2a. To control yaw torque, differential thrust is used i.e., different magnitudes of the thrust of the side propellers cause a moment about the z_b body axis, Fig. 2b.
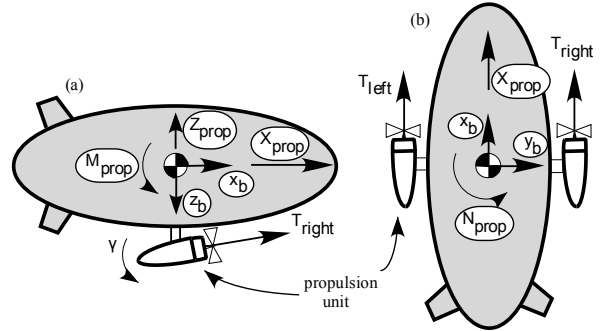
Figure 2. (a) Rotation of the thrust by an angle γ for surge force and pitch torque control. (b) Yaw torque control using differential thrust.

Bow and/or stern thrusters are also used for landing and docking operations.

Below a certain speed limit, aerodynamic surfaces are not effective for control purposes. Then, motion control is achieved by the appropriate use of the propellers: ascending or descending is realized by vectoring the thrust down or up, and heading change by using differential thrust in the port and starboard propeller.

In the following equations of motion, the three control variables are X_{prop} for surge propulsion, M_{prop} for pitch torque, and N_{prop} for yaw torque, [3]. A force Z_{prop} in the z_b axis also appears but its magnitude is very small for normal operating conditions where γ is small. In any case this is a small and bounded disturbance on the nominal – control – model that can be compensated for using a closed loop controller. These terms are functions of the geometrical arrangement of the propulsive units around the body axes as depicted in Fig. 2. The equations that describe the dynamic model are:

$$m_{11}\dot{u}=m_{22}\upsilon r-m_{33}wq+X_u u$$
$$+(B-mg)s\theta+X_{prop} \quad (6a)$$

$$m_{22}\dot{\upsilon}=m_{33}wp-m_{11}ur+Y_\upsilon \upsilon+(mg-B)c\theta s\phi \quad (6b)$$

$$m_{33}\dot{w}=m_{11}uq-m_{22}\upsilon p+Z_w w+(mg-B)c\theta c\phi \quad (6c)$$

$$I_{11}\dot{p}=(I_{22}-I_{33})qr+(m_{22}-m_{33})\upsilon w+K_p p$$
$$+z_{CB}c\theta s\phi B \quad (6d)$$

$$I_{22}\dot{q}=(I_{33}-I_{11})pr+(m_{33}-m_{11})uw+M_q q$$
$$+z_{CB}s\theta B+M_{prop} \quad (6e)$$

$$I_{33}\dot{r}=(I_{11}-I_{22})pq+(m_{11}-m_{22})u\upsilon+N_r r+N_{prop} \quad (6f)$$

A brief explanation of the various terms in (6) follows: m is the vehicle's mass and B is the buoyancy force acting on the CB. The constant z_{CB} is the $z-$ coordinate of the CB; m_{ii}, $i=1,...,3$ are the combined mass and added mass terms; I_{ii}, $i=1,...,3$ are the combined moments and the added moments of inertia terms; X_u, Y_v, Z_w, K_p, M_q, and N_r are the drag, force and moment terms. The lack of control actuation in sway v, heave w, and roll p motions renders the system underactuated.

III. TRAJECTORY PLANNING

In this section, we describe the trajectory planning methodology, i.e., the algorithm that maps an inertial trajectory of the 3D space to body-fixed velocities and orientation. The only restriction on the inertial trajectory is that it must be sufficiently "smooth", i.e., three times differentiable with respect to time.

A. Inertial Trajectory Geometry

We choose the CM of the vehicle as the point of interest. Let us assume that the trajectory which must be tracked by this point is given as a time function of the inertial variables x_R, y_R, z_R and their time derivatives up to the third order. The subscript "R" indicates a reference variable. The position and the magnitude of the velocity vector of a point P on the trajectory are given by

$$\mathbf{s}_P = [x_R, y_R, z_R]^T \qquad (7)$$

$$v_p = \| \mathbf{v}_p \| = \| \dot{\mathbf{s}}_P \| = \sqrt{\dot{x}_R^2 + \dot{y}_R^2 + \dot{z}_R^2} \qquad (8)$$

Of great importance in the derivation is the concept of an orientation frame associated with the curve corresponding to the desired trajectory. To every point of the above curve, we can associate an orthonormal triad of vectors, i.e., a set of unit vectors that are mutually orthogonal, namely, the tangent $\mathbf{e}_t$, the normal $\mathbf{e}_n$, and the binormal $\mathbf{e}_b$, see Fig. 3. Properly arranging these vectors in a 3×3 matrix, we obtain a description of the curve orientation, [9]. The corresponding reference frame is the Frenet-Serret one. The unit vectors are then defined as

$$\mathbf{e}_t = \dot{\mathbf{s}}_P / v_P \qquad (9a)$$

$$\mathbf{e}_b = (\dot{\mathbf{s}}_P \times \ddot{\mathbf{s}}_P) / \| \dot{\mathbf{s}}_P \times \ddot{\mathbf{s}}_P \| \qquad (9b)$$

$$\mathbf{e}_n = \mathbf{e}_b \times \mathbf{e}_t = (\dot{\mathbf{s}}_P \times \ddot{\mathbf{s}}_P) \times \dot{\mathbf{s}}_P / \| \dot{\mathbf{s}}_P \times \ddot{\mathbf{s}}_P \| \| \dot{\mathbf{s}}_P \| \qquad (9c)$$

In the definition of a frame associated with the curve, we use the original definition of the Frenet frame for counterclockwise "rotating" curves; in the case of a clockwise rotating curve, the $z-$ axis of the Frenet frame points in the opposite direction – upwards – than the inertial $\{I\}$ frame. So, in order to define small relative rotation angles for the orientation of a vehicle rotating clockwise and having its z_b- axis pointing downwards, we define a reference frame, associated with the curve as
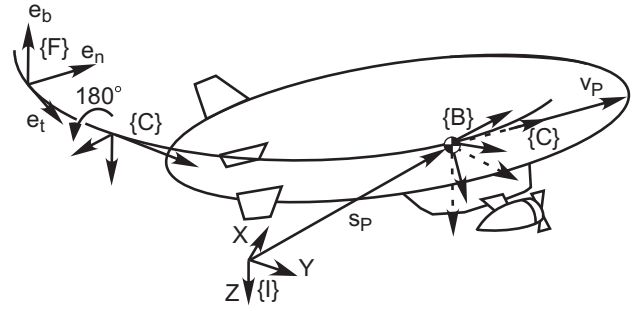
Figure 3. The inertial, the Frenet, the body and the curve frames.

previously, but rotated with respect to the Frenet by an angle of $180°$ about the $x-$ axis of the Frenet frame, Fig. 3. Collectively, we denote the Frenet and the rotated frame as the "curve" frame $\{C\}$.

According to the notation of rotational transformations used in robotics literature [10], we can express the coordinates of a vector given in the curve frame $\{C\}$ to the $\{I\}$ frame with the matrix

$$\mathbf{R}_C^I = [\mathbf{e}_t \quad \mathbf{e}_n \quad \mathbf{e}_b] \qquad (10a)$$

for a counterclockwise rotation, and the matrix

$$\mathbf{R}_C^I = \mathbf{R}_x(180°)[\mathbf{e}_t \quad \mathbf{e}_n \quad \mathbf{e}_b] \qquad (10b)$$

for clockwise rotation. Also, we shall use the fact that

$$\mathbf{R}_I^C = (\mathbf{R}_C^I)^T \qquad (11)$$

In aeronautical applications, it is more convenient to express the various velocities in the current – body – frame, [11]. Thus, the angular velocity of the $\{C\}$ frame with respect to the $\{I\}$ frame expressed in $\{C\}$ frame is given by

$$\mathbf{\Omega}^C = \mathbf{R}_I^C \dot{\mathbf{R}}_C^I \qquad (12a)$$

where $\mathbf{\Omega}^C$ is a skew-symmetric matrix containing the components of the angular velocity vector, and defined as follows:

$$\mathbf{\Omega}^C = \begin{bmatrix} 0 & -\omega_3^C & \omega_2^C \\ \omega_3^C & 0 & -\omega_1^C \\ -\omega_2^C & \omega_1^C & 0 \end{bmatrix} \qquad (12b)$$

From (12b), we collect the components in a vector:

$$\mathbf{\omega}_I^C = [\omega_1^C, \omega_2^C, \omega_3^C]^T = \mathbf{f}_{\omega^C}(\text{traj., variables}) \qquad (13)$$

where "$\mathbf{f}_{\omega^C}(\text{traj., variables})$" means a vector function of the first, second, and third derivatives of the trajectory variables x_R, y_R, z_R.

B. Airship's Dynamics During Tracking

Consider next the dynamics of the robotic airship when its CM tracks accurately the motion of the point P, and let u_R, v_R, w_R, p_R, q_R, r_R denote the reference body-fixed velocities. The magnitude of the total linear velocity vector of the CM is given by

$$v_R = \parallel \mathbf{v}_R \parallel = \parallel [u_R, v_R, w_R]^T \parallel = \sqrt{u_R^2 + v_R^2 + w_R^2} \quad (14)$$

As far as the reference orientation $[\phi_R, \theta_R, \psi_R]^T$ of the body-fixed $\{B\}$ frame with respect to the inertial $\{I\}$ frame is concerned, we have the following: Due to the dynamics, the vehicle $\{B\}$ frame does not coincide with the curve frame $\{C\}$, but undergoes a further rotation with respect to the latter, see Fig. 3, to eventually coincide with the reference – desired – $\{R\}$ frame that provides the orientation consistent with the airship dynamics. Therefore, when the airship CM tracks the curve, the body frame $\{B\}$ coincides with the reference frame $\{R\}$.

The rotation of the $\{B\}$ frame from the $\{C\}$ frame to the $\{R\}$ frame can be expressed using customary aeronautical notation by considering the sideslip angle β and angle of attack α, [12]:

$$\beta = \sin^{-1}(v_R / v_P) \quad (15)$$

$$\alpha = \tan^{-1}(w_R / u_R) \quad (16)$$

The overall rotation is composed by a rotation about body-z_b axis through the angle $-\beta$, followed by a rotation about body-y_b axis through the angle α and is expressed by the matrix.

$$\mathbf{R}_C^R = \mathbf{R}_y^T(\alpha)\mathbf{R}_z^T(-\beta) \quad (17)$$

where the matrix $\mathbf{R}_C^R$ represents the rotation between the $\{C\}$ and the reference or desired frame $\{R\}$. The angular velocity of the $\{R\}$ frame with respect to the $\{C\}$ frame, expressed in $\{R\}$, is computed by

$$\mathbf{\Omega}^R = \mathbf{R}_C^R \dot{\mathbf{R}}_R^C \quad (18)$$

The associated angular velocity vector is as before

$$\mathbf{\omega}_C^R = [\omega_1^R, \omega_2^R, \omega_3^R]^T = \mathbf{f}_{\omega^R}(\text{traj., body variables}) \quad (19)$$

where "$\mathbf{f}_{\omega^R}(\text{traj., body variables})$" means a function of the derivatives of x_R, y_R, and z_R up to the second order as well as of velocities u_R, v_R, w_R and their first order derivatives.

Finally, the reference orientation between the inertial $\{I\}$ frame and the reference $\{R\}$ frame is given by

$$\mathbf{R}_I^R = \mathbf{R}_C^R \mathbf{R}_I^C \quad (20)$$

From (20), we can extract the reference angles using the following, [10]

$$\phi_R = \text{atan2}(r_{23}, r_{33}) \quad (21\text{a})$$

$$\theta_R = \text{atan2}(-r_{13}, \sqrt{r_{23}^2 + r_{33}^2}) \quad (21\text{b})$$

$$\psi_R = \text{atan2}(r_{12}, r_{11}) \quad (21\text{c})$$

where r_{ij} denotes the ij element of $\mathbf{R}_I^R$.

During tracking, the magnitude of the tangent vector to the trajectory $\mathbf{v}_P$ equals the magnitude of the vehicle's velocity vector $\mathbf{v}_R$. From (8) and (14) it is:

$$v_P = v_R \Rightarrow \sqrt{\dot{x}_R^2 + \dot{y}_R^2 + \dot{z}_R^2} = \sqrt{u_R^2 + v_R^2 + w_R^2} \quad (22)$$

From (22) and (8), the reference surge velocity is

$$u_R = \pm\sqrt{\dot{x}_R^2 + \dot{y}_R^2 + \dot{z}_R^2 - v_R^2 - w_R^2} = \pm\sqrt{v_P^2 - v_R^2 - w_R^2} \quad (23)$$

where "$\pm$" indicates that u_R may be positive or negative depending on the direction of the motion; for the remainder we assume forward motion with $u_R > 0$.

Differentiating (23) with respect to time yields,

$$\dot{u}_R = \pm(v_P\dot{v}_P - v_R\dot{v}_R - w_R\dot{w}_R)/\sqrt{v_P^2 - v_R^2 - w_R^2} \quad (24)$$

where $\dot{v}_P$ is given by a simple differentiation of (8). In this way, we have also expressed u_R and $\dot{u}_R$ by the trajectory variables and by v_R, $\dot{v}_R$, w_R, $\dot{w}_R$.

Now, the reference angular velocities are obtained by the succession of the angular velocity of the $\{C\}$ frame with respect to the $\{I\}$ frame and the angular velocity of the reference orientation frame $\{R\}$ with respect to $\{C\}$, all expressed in $\{R\}$:

$$\mathbf{\omega}_I^R = \mathbf{\omega}_C^R + \mathbf{R}_C^R \mathbf{\omega}_I^C = [p_R, q_R, r_R]^T \quad (25)$$

Substituting in (25), the quantities from (13), (17) and (19) and taking into account (23) and (24), we obtain to express the body-frame reference angular velocities as functions of the trajectory variables as well as of the body-fixed variables v_R, $\dot{v}_R$, w_R, $\dot{w}_R$.

Considering now the two unactuated dynamical equations (6b) and (6c) during tracking, and substituting in them the expressions (23), (24), and (25) that give u_R,

$\dot{u}_R$, p_R, q_R, and r_R, a system of two coupled nonlinear time-varying differential equations results:

$$\dot{v}_R = f_v(x_R, \dot{x}_R, \ddot{x}_R, \dddot{x}_R, y_R, \dot{y}_R, \ddot{y}_R, \dddot{y}_R,$$
$$z_R, \dot{z}_R, \ddot{z}_R, \dddot{z}_R, v_R, w_R), \qquad (26)$$
$$v_{R,o} = v_R(t=0)$$

$$\dot{w}_R = f_w(x_R, \dot{x}_R, \ddot{x}_R, \dddot{x}_R, y_R, \dot{y}_R, \ddot{y}_R, \dddot{y}_R,$$
$$z_R, \dot{z}_R, \ddot{z}_R, \dddot{z}_R, v_R, w_R), \qquad (27)$$
$$w_{R,o} = w_R(t=0)$$

Since the time-varying inputs x_R, y_R, z_R, and their derivatives are known, numerical integration of (26) and (27) yields the values of v_R and w_R as functions of time. The actual time needed for a simulated time of $1000 \, s$ is very fast, about $3 \, min$, and the convergence to the reference values is smooth and fast depending on the initial conditions.

Having now these functions, we can go back and compute the rest of the reference variables: u_R from (23), p_R, q_R and r_R from (25), and ϕ_R, θ_R, and ψ_R from (21). Therefore, at this step, all feasible trajectory variables are known.

IV. OPEN-LOOP CONTROL AND SIMULATIONS

In this section, we design an open-loop controller in order for the robotic airship to track a reference trajectory. Then, simulation results are presented to illustrate the way the above planning methodology applies.

A. Open-Loop Control Inputs

Once the body-fixed variables, i.e., linear and angular velocities and Euler angles, required for the airship to track the reference trajectory have been computed, it is straightforward to construct the corresponding open-loop controls using the dynamic model. Indeed, from (6a), (6e), and (6f) it is respectively:

$$X_{prop,R} = m_{11}\dot{u}_R - m_{22}v_R r_R + m_{33}q_R w_R$$
$$- X_u u_R + (mg - B)s\theta_R \qquad (28a)$$

$$M_{prop,R} = I_{22}\dot{q}_R + (I_{11} - I_{33})p_R r_R +$$
$$(m_{11} - m_{33})u_R w_R - M_q q_R - z_{CB}s\theta_R B] \qquad (28b)$$

$$N_{prop,R} = I_{33}\dot{r}_R + (I_{22} - I_{11})p_R q_R +$$
$$(m_{22} - m_{11})u_R v_R - N_r r_R \qquad (28c)$$

In the case of tracking with constant reference velocities $\dot{u}_R$, $\dot{q}_R$, and $\dot{r}_R$ are zero; else, one must take surge acceleration from (24), and differentiate q_R and r_R from (25).

The presented trajectory planning algorithm and the direct resulted open-loop controller may be incorporated in a two-step, closed-loop, trajectory-tracking controller design. Forward feeding the actuators of an airship with the above computed open-loop controls, consistent with

vehicle dynamics, one can design a feedback controller to take care of the small remaining errors. Such a controller will not require high gains and, hence, will have an improved performance. A further advantage of the method is the ease of checking the possibility that the computed controls result in actuator saturation; if this is the case, the designer can replan the trajectory choosing slower functions of time for the representation of the inertial curve. Moreover, we observe that this methodology can be applied to vehicles with similar dynamic models and actuation, such as unmanned airplanes and helicopters, moving in 3D space.

B. Simulation Results

In this section, we present an example of trajectory planning and open-loop controlled motion. The CM inertial trajectory is a helix given by:

$$x_R(t) = 30\cos(0.01t) \qquad (29a)$$

$$y_R(t) = 30\sin(0.01t) \qquad (29b)$$

$$z_R(t) = 0.025t \qquad (29c)$$

Differentiating (29) three times and following the above designed trajectory planning procedure, provides the reference variables which are depicted in the following diagrams in dotted lines; the actual variables are given in solid lines. Since there is no error feedback in the open-loop controls, we must start the simulation using the reference initial values for the airship dynamics in order for the application to make sense.

In Fig. 4, the planned reference and the generated path are depicted. In Fig. 5, the angles α and β computed from (15) and (16) are shown. In Fig. 6, the constant values of the surge force and the torques in pitch and yaw motions computed from (28) are shown. Fig. 7 shows a perfect inertial path following of the reference position for the CM of the airship. As far as the reference orientation concerns, negligible errors are only present in the roll Euler angle. Such errors are attributed to numerical errors and to inaccurate setting the initial values for the simulation. Fig. 8 depicts reference and resulting linear and angular velocities. It can be seen that they match each other very well.
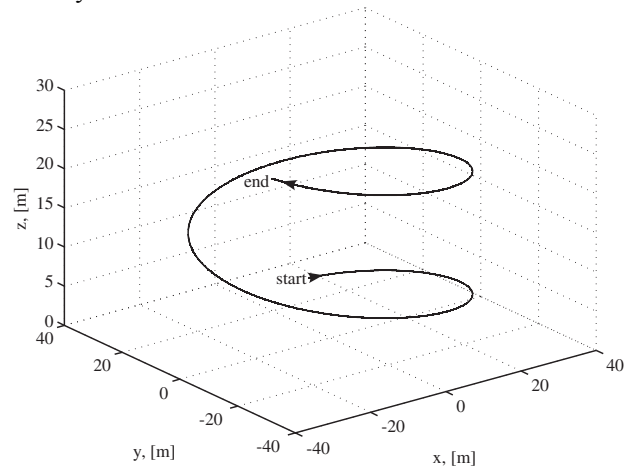
Figure 4.   The actual and the reference 3D path.
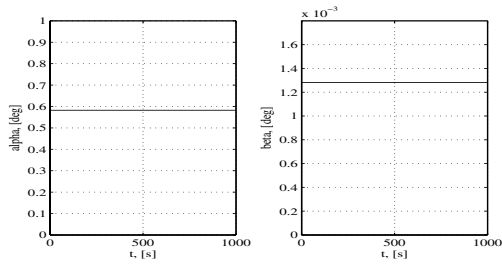
Figure 5.   The angles α and β .
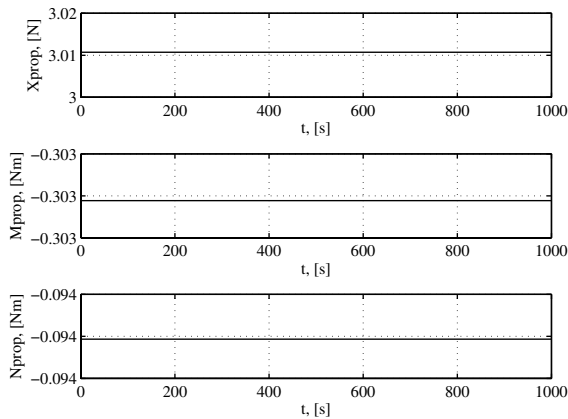
Figure 6.   Open-loop control inputs.
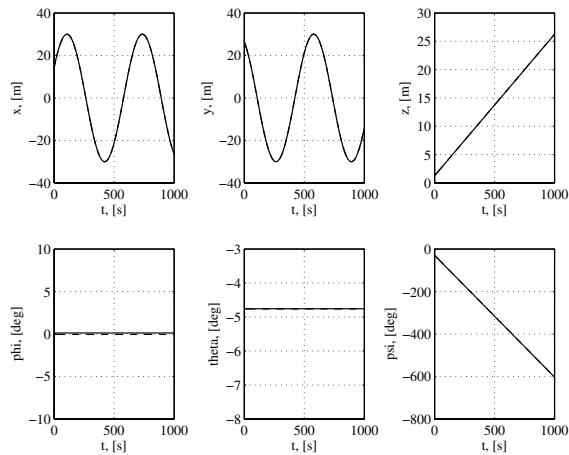
Figure 7.   Inertial position variables of the CM and the Euler angles.
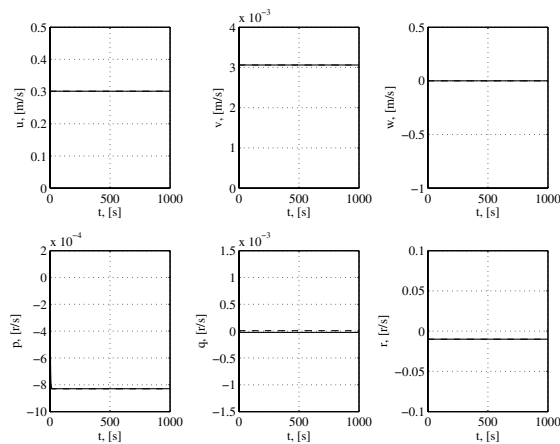
Figure 8. Body-fixed linear and angular velocities.

V.   CONCLUSIONS

In this paper, we described a method for planning six DOF trajectories for an underactuated unmanned airship and for computing the open-loop controls. Beginning with a smooth inertial 3D trajectory to be tracked by the center of mass of the vehicle, the proposed algorithm, based on the dynamics of the system, provides the 3D corresponding body-fixed linear and angular velocities and the vehicle orientation, yielding a feasible 6 DOF trajectory. The derived trajectory is further used to compute the three available open-loop controls required to follow the trajectory. Finally, simulation results are presented to demonstrate the effectiveness of the algorithm.

For future work, we consider the design of a robust closed-loop controller in order to counteract parametric uncertainties and environmental disturbances. Also, to avoid Euler angle representational singularities, the representation of kinematics by means of quaternions will be considered.

REFERENCES

[1]   G. A. Khoury and J. D. Gillet, *Airship Technology*. Cambridge University Press, 1999.

[2]   A. Elfes, et. al., "Robotic airships for exploration of planetary bodies with an atmosphere: autonomy challenges," in *Autonomous Robots,* vol. 14, pp. 147-164, July 2003.

[3]   S. B. V. Gomes and J. J. Ramos, "Airship dynamic modeling for autonomous operation," *IEEE International Conference on Robotics and Automation,* Leuven, Belgium, May 1998.

[4]   L. Beji and A Abichou,, "Tracking control of trim trajectories of a blimp for ascent and descent flight maneuvers," in *International Journal of Control,* vol. 78, pp. 706-719, July 2005.

[5]   J. R. Azinheira, et. al., "Visual servo control for the hovering of an outdoor robotic airship," *IEEE International Conference on Robotics and Automation,* Washington DC, USA, May 2002.

[6]   R. Mahony, and T. Hamel, "Robust trajectory tracking for a scale model autonomous helicopter," in *International Journal of Robust and Nonlinear Control,* vol. 14, pp. 1035-1059, 2004.

[7]   F. Repoulias and E. Papadopoulos, "On spatial trajectory planning and open-loop control design for underactuated AUVs," *IFAC Symposium on Robot Control,* Bologna, Italy, September 2006.

[8]   F. Repoulias and E. Papadopoulos, "Trajectory planning and tracking control of underacuated AUVs," *IEEE International Conference on Robotics and Automation,* Barcelona, Spain, April 2005, pp. 1622-1627.

[9]   J. Angeles, *Fundamentals of Robotic Mechanical Systems. Theory, Methods, and Algorithms.* Springer, New York, 1997.

[10]   L. Sciavico and B. Siciliano, *Modeling and Control of Robot Manipulators.* McGraw-Hill, USA, 1996.

[11]   H. Baruh, *Analytical Dynamics.* McGraw-Hill, Singapore, 1999.

[12]   G. M. Siouris, *Missile Guidance and Control Systems.* Springer, New York, 2004.